Stencils with Isotropic Discretization Error for Differential Operators

Michael Patra, Mikko Karttunen

Biophysics and Statistical Mechanics Group, Laboratory for Computational Engineering, Helsinki University of Technology, 02015 Hut, Finland

We derive stencils, i.e., difference schemes, for differential operators for which the discretization error becomes isotropic in the lowest order. We treat the Laplacian, Bilaplacian (=biharmonic operator), and the gradient of the Laplacian both in two and three dimensions. For three dimensions $\mathcal{O}(h^2)$ results are given while for two dimensions both $\mathcal{O}(h^2)$ and $\mathcal{O}(h^4)$ results are presented. The results are also available in electronic form as a Mathematica file. It is shown that the extra computational cost of an isotropic stencil usually is less than 20%.   © 2005 Wiley Periodicals, Inc. Numer Methods Partial Differential Eq 22: 936–953, 2006

I. INTRODUCTION

The most general form of a partial differential equation (PDE) is

$$\mathcal{D}f(x_1, \ldots, x_N) = 0, \tag{1.1}$$

where $\mathcal{D}$ is a differential operator and $(x_1, \ldots, x_N) \in \Omega, \Omega \subset \mathbb{R}^N$. If $\mathcal{D}$ is linear in its argument, the PDE is called linear. For a unique solution, Eq. (1.1) has to be supplemented by pure boundary, pure initial, or mixed initial-boundary conditions.

Every PDE can always be solved in the following way: The PDE is discretized, i.e., both the differential operator $\mathcal{D}$ and the boundary and/or initial conditions are discretized on a grid. The discretization of $\mathcal{D}$ is called a finite-difference scheme (FDS) $\mathcal{S}$. Assuming a regular grid with spacing h, $\mathcal{S}$ can be represented by a matrix S called a "stencil,"

$$\mathcal{D}f(x_1, \ldots, x_N) \approx \sum_{i_1 \ldots i_N = -r}^{r} S_{i_1 \ldots i_N} f(x_1 + i_1 h, \ldots, x_N + i_N h). \tag{1.2}$$

The size of the matrix S is $2r + 1$. A stencil with $r = 1$ is called a compact stencil. A stencil is diagonally dominant iff

$$|S_{0,\dots,0}| \geq \sum_{i_1\dots i_N=-r}^{r}{}' \; |S_{i_1\dots i_N}|, \tag{1.3}$$

where the prime denotes that the element $S_{0,\dots,0}$ is omitted from the summation. Application of $\mathcal{D}$ to a constant function f gives $\sum_{i_1\dots i_N} S_{i_1\dots i_N} = 0$, and a stencil thus is diagonally dominant iff $S_{0,\dots,0}$ is nonzero and the sign of all other coefficients $S_{i_1\dots i_N}$ is opposite to $S_{0,\dots,0}$.

Application of Eq. (1.2) to Eq. (1.1) gives one equation for each grid point in Ω. If the PDE is linear, the discretization of Eq. (1.1) thus gives a system of linear equations, described by some matrix M which is banded and sparse. The computational load lies almost exclusively in solving this set of equations. Consequently, most of the published work on finite-difference schemes focuses on the needs of the linear-equation solver, i.e., on finding an S that minimizes the work for the linear-equation solver. In particular, the numerical work per grid point depends on the band width of M (which increases with r), giving a strong preference for compact stencils. In addition, standard linear-equation solvers only converge if M is diagonally dominant [1, pp 122 and 158; 2, p 151]. The numerical need to use stencils that are both compact and diagonally dominant is very strong, and one is willing to go into extra effort in order to be able to use such stencils (see Section VII). The concepts of compactness and diagonal dominance are closely related as a noncompact stencil cannot be diagonally dominant. This is most easily seen by considering a function $f(x_1, \dots, x_N)$ that depends only on x_1. Application of S then results in a one-dimensional finite-difference scheme for which it is known that its coefficients have alternating sign [3]. For $r > 1$, this violates the assumption of diagonal dominance as there all coefficients (except for the one in the centre) have the same sign [cf. Eq. (1.3)].

The approach of discretizing all variables and subsequently (explicitly or implicitly) solving a system of (linear) equations can always be applied. However, for many important PDEs the differential operator separates into $\mathcal{D}_t$, acting only onto the "time" t, and $\mathcal{D}$, acting on the "spatial" variables $x_1, \dots, x_N$,

$$(\mathcal{D}_t + \mathcal{D}) f(t, x_1, \dots, x_N) = 0 \tag{1.4}$$

in $[a; \infty) \times \Omega, \Omega \subset \mathbb{R}^N$, where the dimension N is decreased by 1 compared to the dimension N used in the general case (1.1) as one dimension has been split off and separated into the variable t. Initial conditions are specified at $t = a$, i.e., for $(a, x_1, \dots, x_N) \, \forall \, (x_1, \dots, x_N) \in \Omega$, and boundary conditions for the spatial variables, i.e., for $(t, x_1, \dots, x_N) \, \forall \, t \in [a; \infty), (x_1, \dots, x_N) \in \partial\Omega$. As a rule of thumb, PDEs modelling dynamical processes [6] are of the form (1.4), whereas PDEs modelling static processes are not. Usually parabolic PDEs (e.g., the diffusion equation) and hyperbolic PDEs (e.g., the wave equation) are of form (1.4), whereas elliptic PDEs (e.g., Poisson's equation) rarely are.

Equations of type (1.4) are much easier to solve than the general case (1.1). Because the differential operator separates into $\mathcal{D}_t$ and $\mathcal{D}$, only the spatial region Ω needs to be discretized, resulting in a set of ODEs with t as independent variable. As all initial conditions are specified at $t = a$, the set of ODEs can be solved with a standard integrator (e.g., Runge–Kutta or extrapolation methods) by integrating in t. Integrating sets of ODEs with initial conditions is much more efficient than solving general PDEs [2].

In the general case (1.1), application of a stencil results in a system of equations that need to be solved. If the differential operator $\mathcal{D}$ is nonlinear, these equations are nonlinear, too, complicating

the process of computing a solution further. Even for a linear differential operator $\mathcal{D}$, the linear equation solver imposes restrictions on $\mathcal{S}$ (such as diagonal dominance; see above). None of these problems arises for the case (1.4) as no solution of a set of equations is needed. In particular, there thus is no difference between linear and nonlinear PDEs, and there is no need for the stencil to be diagonally dominant or compact. As we will show in Section VI, the computational cost depends only lightly on r, and noncompact stencils (i.e., $r > 1$) can be attractive. Thus, the development of finite-difference schemes can now focus on accuracy. Only little work has been published on this, probably because the problem seems to be a very easy one. As we will show, this is not the case. With this article we intend to fill this gap, and we will focus entirely on PDEs of form (1.4).

II. ANISOTROPY

Discretization of a differential operator with finite grid size h inadvertently leads to a truncation error that decreases with h as $\mathcal{O}(h^n)$,

$$\mathcal{D}f(x_1,\ldots,x_N) = \mathcal{S}f(x_1,\ldots,x_N) + \mathcal{O}(h^n), \qquad (2.1)$$

and n is called the order of the stencil. The order n is frequently used as a measure of the "quality" of a finite-difference scheme. However, Eq. (2.1) contains only the first term in a series expansion in terms of h,

$$\mathcal{D}f(x_1,\ldots,x_N) = \mathcal{S}f(x_1,\ldots,x_N) + h^n g(x_1,\ldots,x_N) + h^{n+1} g^{(n+1)}(x_1,\ldots,x_N) + h^{n+2} \cdots. \qquad (2.2)$$

Comparison of Eqs. (2.1) and (2.2) shows that $g(x_1,\ldots,x_N)$ gives the leading error term, i.e., the truncation error in lowest nonvanishing order of h. The function g depends on $\mathcal{D}, \mathcal{S}$, and f, and can therefore be written as $g = \tilde{\mathcal{D}}f$ where $\tilde{\mathcal{D}}$ is some (differential) operator. There can be several finite-difference schemes $\mathcal{S}$ of the same order n for the same differential operator $\mathcal{D}$ that differ in their truncation error, namely by differing in $\tilde{\mathcal{D}}$.

The important point now is that not all truncation errors are equivalently important. While a small error in $f(t,\vec{r})$ might be acceptable as long as it is below some threshold, it might be much less acceptable if $f(t,\vec{r})$ no longer fulfils all symmetry or conservation laws of the system. For the integration of Newton's equation of motion for conservative (i.e., energy-conserving) systems this was realized already a long time ago and addressed by proper algorithms. The leap-frog and equivalent algorithms are only second-order accurate in the positions and momenta but the more-important energy of the system is conserved to fourth order in the time step (see Ref. 4 and references therein).

A more general class of problems is characterized by symmetry requirements. In particular, many (if not most) systems are spatially isotropic, i.e., $\mathcal{D}$ has no preferred directions. The underlying grid, however, has, namely the directions of its axes. These directions may or may not show up in the truncation error $\tilde{\mathcal{D}}$. We will call a finite-difference scheme "isotropic" if the leading error term does not have preferred directions and "anisotropic" otherwise. This is a "local" property, i.e., it is local in space and with respect to a single integration time step.

We will demonstrate now that this local property is relevant for the global properties of the solution. As an easy example, we consider the two-dimensional diffusion equation with spherically symmetric absorbing boundary conditions,

$$\frac{\partial f(t,\vec{r})}{\partial t} = \Delta f(t,\vec{r}), \qquad f(t,\vec{r}) = 0 \quad \forall\, |\vec{r}| \geq 2. \qquad (2.3)$$
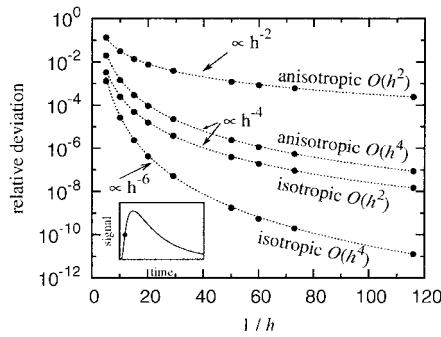
FIG. 1.   Relative difference between $f(t_{1/2}, \vec{r}_1)$ and $f(t_{1/2}, \vec{r}_2)$. The inset shows the solution of the PDE at $\vec{r}_1$ and the time $t_{1/2}$ where it has reached half its maximum. The lines are power-laws, as given by the labelling. The points are computed by numerical solution of the corresponding ODEs.

The system is excited by a pulse at the origin, $f(t, \vec{r}) = \delta(\vec{r})\delta(t)$. We consider the response at two points $\vec{r}_i$, with same separation from the origin, $|\vec{r}_1| = |\vec{r}_2| = 1$, but different orientation: $\vec{r}_1 = (1, 0)$ and $\vec{r}_2 \approx (1/\sqrt{2}, 1/\sqrt{2})$. Since both $\vec{r}_1$ and $\vec{r}_2$ have to be on a grid point to ensure $|\vec{r}_1| = |\vec{r}_2| = 1$, there is only a limited number of choices [for example, $\vec{r}_2 = (21/29, 20/29)$ with grid spacing $h = 1/29$].

Equation (2.3) was discretized in space by application of a finite different scheme. We have used isotropic and anisotropic $\mathcal{O}(h^2)$ and $\mathcal{O}(h^4)$ stencils from Section V. Since for the Laplacian, terms $\mathcal{O}(h^n)$ with odd n vanish in the series expansion (2.2), the next nonvanishing term, the anisotropic component of the truncation error, is an order h^2 higher than the leading term of the truncation error. The resulting system of ordinary differential equations was integrated using a fourth-order Runge-Kutta algorithm. The time step was verified to be short enough that further reduction would not change the results. The inset in Fig. 1 shows that $f(t, \vec{r}_i)$ first rises quickly and then drops of slowly. For the analysis, we used the time $t_{1/2}$ when $f(t, \vec{r}_i)$ has reached half of its maximum value.

Figure 1 shows the relative deviation between f at points $\vec{r}_1$ and $\vec{r}_2$ as a function of grid spacing h. Since $|\vec{r}_1| = |\vec{r}_2|$, these values should be identical, and any deviation thus is a direct violation of the isotropy property of the system induced by the grid. As Fig. 1 shows, for the $\mathcal{O}(h^n)$ stencils that we have labelled as "anisotropic" the relative anisotropy is of order $\mathcal{O}(h^n)$, too, whereas for the "isotropic" stencils the relative anisotropy is of order $\mathcal{O}(h^{n+2})$, i.e., the order has an additional factor h^2. This means the local improvement is directly reflected in the global result. This gives another justification for the terms isotropic and anisotropic stencils.

In reaction-diffusion models (see, e.g., Ref. 5) and the so-called phase field models [6] the grid spacing h is usually chosen to be $1/10$ to $1/20$ of the size of the smallest structures in the system, such that the relative anisotropy can be as large as 10^{-1} if a low-order anisotropic stencil is chosen. As we will show in Section VI, the additional computational cost for using better stencils is negligible, and one can thus reduce the relative anisotropy of the computed result by several magnitudes almost without any increase in computational cost.

III. DEFINITIONS

In this article we consider the Laplacian, the Bilaplacian (also known as biharmonic operator), and the gradient of the Laplacian. For the latter it is sufficient to treat only the x-component.

The three operators and our notation for them is as follows:

$$\Delta = \frac{\partial^2}{\partial x^2} + \frac{\partial^2}{\partial y^2} + \frac{\partial^2}{\partial z^2}, \qquad \Delta^2 = \left[\frac{\partial^2}{\partial x^2} + \frac{\partial^2}{\partial y^2} + \frac{\partial^2}{\partial z^2}\right]^2,$$

$$\frac{\partial}{\partial x}\Delta = \frac{\partial^3}{\partial x^3} + \frac{\partial^3}{\partial x\partial y^2} + \frac{\partial^3}{\partial x\partial z^2}. \tag{3.1}$$

To obtain the two-dimensional versions of the operators, all derivatives with respect to z are omitted.

We present the stencils $\mathcal{S}$ by giving the coefficients of the matrix S. S_{ijk} gives the prefactor of the stencil for the term $f(x + ih, y + jh, z + kh)$. The coefficients are displayed in the order

$$\begin{bmatrix} S_{1,1,-1} & S_{0,1,-1} & S_{-1,1,-1} \\ S_{1,0,-1} & S_{0,0,-1} & S_{-1,0,-1} \\ S_{1,-1,-1} & S_{0,-1,-1} & S_{-1,-1,-1} \end{bmatrix} \begin{bmatrix} S_{1,1,-0} & S_{0,1,-0} & S_{-1,1,-0} \\ S_{1,0,-0} & S_{0,0,-0} & S_{-1,0,-0} \\ S_{1,-1,-0} & S_{0,-1,-0} & S_{-1,-1,-0} \end{bmatrix} \begin{bmatrix} S_{1,1,-1} & S_{0,1,-1} & S_{-1,1,-1} \\ S_{1,0,-1} & S_{0,0,-1} & S_{-1,0,-1} \\ S_{1,-1,-1} & S_{0,-1,-1} & S_{-1,-1,-1} \end{bmatrix}.$$

$$\tag{3.2}$$

In other words, each two-dimensional matrix corresponds to one fixed value for z, and x is larger on the left than on the right. (These definitions are only relevant when discussing the gradient of the Laplacian because all other stencils are completely symmetric.)

Each "general" stencil $\mathcal{S}$ is defined by a set of conditions for its coefficients that will turn out to be a set of linear equations. "Specific" stencils can be obtained by setting certain coefficients to zero. One aim can be to minimise the number of nonzero elements n_1. Elements in the interior of the stencil might be accessed by the cpu even if they have the value zero. For this reason, we also introduce the number n_2, denoting the number of elements that are either nonzero or are surrounded by nonzero elements.

Apart from the linear equations for the general stencils, in the following we will also give the coefficients for the specific stencils with minimal n_1 or n_2. To aid the reader, a small graphic is displayed showing that stencil. Nonzero elements are indicated by a filled square (■). If a zero is lying between two nonzero elements (and hence is included in the count n_2), it is denoted by an open square (□). Other zeros are marked by a centered dot (·).

IV. METHOD

A stencil $\mathcal{S}$ is an $\mathcal{O}(h^n)$ approximation for a differential operator $\mathcal{D}$ of order p if and only if it gives the correct result for any polynomial $P_q(x, y)$ of order $q = p + n - 1$, i.e.,

$$\sum_{ij} S_{ij} P_q(x + ih, y + jh) = \mathcal{D}P_q(x, y) \qquad \text{with} \quad P_q(x, y) = \sum_{i,j=0\ldots q}^{i+j\leq q} a_{ij} x^i y^j, \tag{4.1}$$

is fulfilled for all possible values of $\{a_{ij}\}, x, y,$ and h. For convenience the equations are given only for the two-dimensional case. The three-dimensional case is equivalent. $\mathcal{D}P_q(x, y)$ is easily computed analytically, such that Eq. (4.1) is well defined.

S is a $(2r + 1) \times (2r + 1)$-matrix, and r is the smallest integer such that $2r + 1 \geq p + n - 1$. The amount of work is reduced significantly if S is decomposed into m independent elements

connected by symmetry. For example, the Laplacian is invariant under $x \leftrightarrow -x$, $y \leftrightarrow -y$, and/or $x \leftrightarrow y$. Thus, S contains only $m = 3$ independent elements,

$$S = \begin{bmatrix} c_1 & c_2 & c_1 \\ c_2 & c_3 & c_2 \\ c_1 & c_2 & c_1 \end{bmatrix}. \tag{4.2}$$

The stencils derived in this article contain between 3 and 12 independent elements.

Inserting Eq. (4.2) into Eq. (4.1) and demanding the equality of left-hand and right-hand sides for all possible values of $\{a_{ij}\}$, x, y, and h gives all sufficient and necessary conditions among the coefficients $c_1, \ldots, c_m$.

Unfortunately, current symbolic algebra software does not seem to be able to handle a direct automatic solution of Eq. (4.1). The problem is that they are designed to compute solutions $\{c_i\}$ of Eq. (4.1) as a function of $\{a_{ij}\}$, x, y, and h, whereas we need to find the "special" solutions $\{c_i\}$ of Eq. (4.1) that are independent of $\{a_{ij}\}$, x, y, and h.

We thus replace the single equation (4.1) by the equivalent system of equations

$$\sum_{ij} S_{ij}(x + ih)^k(y + jh)^l - \mathcal{D}[x^k y^l] = 0 \qquad \forall\, 0 \leq k, l, \quad k + l \leq q. \tag{4.3}$$

In each equation of this system of equations, the factors in front of h, x, and y separately need to equate to zero. The advisable way of proceeding is as follows: An equation without x and y is picked by hand and solved for, e.g., c_1. This gives $c_1 = c_1(c_2, \ldots, c_m)$. Substitution into all equations and repeating this procedure gives $c_2 = c_2(c_3, \ldots, c_m), c_3 = c_3(c_4, \ldots, c_m)$, and so forth, until after finding and inserting the solution for c_k, all equations become identically true ($k \leq m$). Backsubstitution then gives $c_i = (c_{k+1}, \ldots, c_m), i = 1, \ldots, k$. If $k = m$, the stencil is determined uniquely. Otherwise, the freedom to choose $m - k$ coefficients arbitrarily still exists.

The procedure to pick a suitable equation can be automatised, but since for the stencils presented in this article no more than 10 iterations are needed, we refrained from doing so, and picked the equations by hand. The solution, insertion and simplification were done using the symbolic algebra package Mathematica version 3. (We also tried version 4 but for this particular purpose it seemed to be slower.)

The procedure presented above allows a systematic derivation of the conditions among the coefficients $c_1, \ldots, c_m$ describing a general stencil. Usually $k < m$ such that there is freedom to set some of the coefficients to specific values (in practice to 0) to yield specific stencil with desirable properties.

Equation (4.1) defines only the order of the truncation error but does not impose any conditions on its form. A stencil is isotropic if and only if its leading error term is isotropic and thus is described by some differential isotropic operator $\tilde{\mathcal{D}}$. Equation (4.1) thus has to be amended to

$$\sum_{ij} U(\omega) S_{ij} P_{q+p'}(x + ih, y + jh) = \mathcal{D}P_{q+p'}(x, y) - h^n \tilde{\mathcal{D}} P_{q+p'}(x, y) + \mathcal{O}(h^{n+p'}), \tag{4.4}$$

where p' is the order of the differential operator $\tilde{\mathcal{D}}$, and $U(\omega)$ rotates the matrix S by the angle ω. The same procedure as described above is applied again, with one exception: the solution $\{c_i\}$ has to be independent not only of x, y, and h but also of ω. The ω-independence of the leading error term is the general definition for an isotropic stencil that works also for operators [such as $(\partial/\partial x)\Delta$] that themselves have a preferred direction. We found that for given $\mathcal{D}$ and n, all

isotropic stencils have the same $\tilde{\mathcal{D}}$ but have not been able to prove that this is also the case if other $\mathcal{D}$ than the ones studied in this article are used.

Symbolic algebra software seems to have been used only very recently to derive finite-difference schemes for differential operators. To the best of our knowledge, the idea was first used by Gupta and coworkers [8], but their approach is somewhat different from ours. They start with two sets of equations. The first set equates, in our notation, the values of the function $f(x + ih, y + jh)$ at all points of the stencil to the values of the polynomial $P_q(x + ih, y + jh)$. The second set relates the coefficients a_{ij} of the polynomial to the differential operator and certain of its higher derivatives. Solving the complete set of equations gives the coefficients of the stencil, as well as an expression for the truncation error in terms of a_{ij} and the higher derivatives of the differential operator. In this approach, one needs to decide *a priori* which coefficients of the stencil should be nonzero, and their precise choice determines the truncation error of the stencil. Unfortunately, there is no easy relation between the choice of nonzero coefficients and the properties of the stencil making this method feasible mainly for small (=compact) stencils.

V. RESULTS

First, we define the shapes of the stencils of different order. We then give the necessary and sufficient conditions among the coefficients $\{c_i\}$ that all stencils have to fulfil. This is followed by the stronger conditions for stencils with isotropic truncation error. Finally, we present a few specific stencils that have useful properties. Whenever we managed to find a previous publication of such a stencil, we have provided the references. All stencils are available as Mathematica file from our website http://www.softsimu.org/downloads.shtml. This file contains not only the stencils but also routines that will automatically check that the stencils indeed fulfil the relevant conditions.

A. $\mathcal{O}(h^2)$ Stencils for the Two-dimensional Laplacian

$$\Delta f(x, y) = \frac{1}{h^2} \begin{bmatrix} c_1 & c_2 & c_1 \\ c_2 & c_3 & c_2 \\ c_1 & c_2 & c_1 \end{bmatrix} + \mathcal{O}(h^2). \tag{5.1}$$

General stencils are given by

$$c_2 = 1 - 2c_1, \qquad c_3 = 4c_1 - 4. \tag{5.2}$$

There is only a single isotropic stencil. It has truncation error $(h^2/12)\Delta^2 f(x, y) + \mathcal{O}(h^4)$.

c_1	c_2	c_3	n_1	n_2	Stencil	Ref.
0	1	-4	5	5	Ani	See any textbook
$\frac{1}{6}$	$\frac{2}{3}$	$-\frac{10}{3}$	9	9	Iso	Known under the name "Mehrstellen"

Ani, anisotropic; Iso, isotropic.

Shapes of these stencils from top to bottom:

B. $\mathcal{O}(h^4)$ Stencils for the Two-dimensional Laplacian

$$\Delta f(x, y) = \frac{1}{h^2} \begin{bmatrix} c_1 & c_2 & c_3 & c_2 & c_1 \\ c_2 & c_4 & c_5 & c_4 & c_2 \\ c_3 & c_5 & c_6 & c_5 & c_3 \\ c_2 & c_4 & c_5 & c_4 & c_2 \\ c_1 & c_2 & c_3 & c_2 & c_1 \end{bmatrix} + \mathcal{O}(h^4). \tag{5.3}$$

General stencils are given by

$$c_3 = -\tfrac{1}{12} - 2c_1 - 2c_2, \qquad c_4 = -16c_1 - 8c_2,$$
$$c_5 = \tfrac{4}{3} + 32c_1 + 14c_2, \qquad c_6 = -5 - 60c_1 - 24c_2. \tag{5.4}$$

Isotropic stencils are given by

$$c_2 = -\tfrac{1}{30} - 4c_1, \qquad c_3 = 6c_1 - \tfrac{1}{60}, \qquad c_4 = \tfrac{4}{15} + 16c_1,$$
$$c_5 = \tfrac{13}{15} - 24c_1, \qquad c_6 = 36c_1 - \tfrac{21}{5}. \tag{5.5}$$

For all isotropic stencils, the truncation error is $(h^2/90) \, \Delta^3 f(x, y) + \mathcal{O}(h^6)$.

c_1	c_2	c_3	c_4	c_5	c_6	n_1	n_2	Stencil	Ref.
0	0	$-\tfrac{1}{12}$	0	$\tfrac{4}{3}$	-5	9	9	Ani	7
$-\tfrac{1}{120}$	0	$-\tfrac{1}{15}$	$\tfrac{2}{15}$	$\tfrac{16}{15}$	$-\tfrac{9}{2}$	17	25	Iso	
0	$-\tfrac{1}{30}$	$-\tfrac{1}{60}$	$\tfrac{4}{15}$	$\tfrac{13}{15}$	$-\tfrac{21}{5}$	21	21	Iso	

Ani, anisotropic; Iso, isotropic.

Shapes of these stencils from top to bottom:

C. $\mathcal{O}(h^2)$ Stencils for the Three-dimensional Laplacian

$$\Delta f(x, y, z) = \frac{1}{h^2} \begin{bmatrix} c_1 & c_2 & c_1 \\ c_2 & c_3 & c_2 \\ c_1 & c_2 & c_1 \end{bmatrix} \begin{bmatrix} c_2 & c_3 & 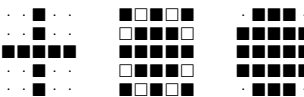c_2 \\ c_3 & c_4 & c_3 \\ c_2 & c_3 & c_2 \end{bmatrix} \begin{bmatrix} c_1 & c_2 & c_1 \\ c_2 & c_3 & c_2 \\ c_1 & c_2 & c_1 \end{bmatrix} + \mathcal{O}(h^2). \tag{5.6}$$

General stencils are given by

$$c_3 = 1 - 4c_1 - 4c_2, \qquad c_4 = 16c_1 + 12c_2 - 6. \tag{5.7}$$

Isotropic stencils are given by

$$c_2 = \tfrac{1}{6} - 2c_1, \qquad c_3 = \tfrac{1}{3} + 4c_1, \qquad c_4 = -4 - 8c_1. \tag{5.8}$$

For all isotropic stencils, the truncation error is $(h^2/12)\,\Delta^2 f(x, y, z) + \mathcal{O}(h^4)$.

c_1	c_2	c_3	c_4	n_1	n_2	Stencil	Ref.
0	0	1	-6	7	7	Ani	See any text book
$\frac{1}{12}$	0	$\frac{2}{3}$	$-\frac{14}{3}$	15	27	Iso	8
0	$\frac{1}{6}$	$\frac{1}{3}$	-4	19	19	Iso	9
$-\frac{1}{12}$	$\frac{1}{3}$	0	$-\frac{10}{3}$	21	27	Iso	8
$\frac{1}{30}$	$\frac{1}{10}$	$\frac{7}{15}$	$-\frac{64}{15}$	27	27	Iso	10

Ani, anisotropic; Iso, isotropic.

Shapes of these stencils from top to bottom:

D. $\mathcal{O}(h^2)$ Stencils for the Two-dimensional Bilaplacian

$$\Delta^2 f(x, y) = \frac{1}{h^4} \begin{bmatrix} c_1 & c_2 & c_3 & c_2 & c_1 \\ c_2 & c_4 & c_5 & c_4 & c_2 \\ c_3 & c_5 & c_6 & c_5 & c_3 \\ c_2 & c_4 & c_5 & c_4 & c_2 \\ c_1 & c_2 & c_3 & c_2 & c_1 \end{bmatrix} + \mathcal{O}(h^2). \tag{5.9}$$

General stencils are given by

$$c_3 = 1 - 2c_1 - 2c_2, \qquad c_4 = 2 - 16c_1 - 8c_2,$$
$$c_5 = 32c_1 + 14c_2 - 8, \qquad c_6 = 20 - 60c_1 - 24c_2. \tag{5.10}$$

Isotropic stencils are given by

$$c_2 = \tfrac{1}{3} - 4c_1, \qquad c_3 = \tfrac{1}{3} + 6c_1, \qquad c_4 = 6c_1 - \frac{2}{3},$$
$$c_5 = -\tfrac{10}{3} - 24c_1, \qquad c_6 = 12 + 36c_1. \tag{5.11}$$

For all isotropic stencils, the truncation error is $(h^2/6)\,\Delta^3 f(x, y) + \mathcal{O}(h^4)$.

c_1	c_2	c_3	c_4	c_5	c_6	n_1	n_2	Stencil
0	0	1	2	-8	20	13	13	Ani
$\frac{1}{12}$	0	$\frac{5}{6}$	$\frac{2}{3}$	$-\frac{16}{3}$	15	17	25	Iso
0	$\frac{1}{3}$	$\frac{1}{3}$	$-\frac{2}{3}$	$-\frac{10}{3}$	12	21	21	Iso

Ani, anisotropic; Iso, isotropic.

Shapes of these stencils from top to bottom:
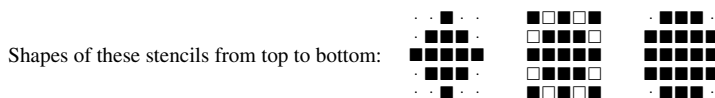
E. $\mathcal{O}(h^4)$ Stencils for the Two-dimensional Bilaplacian

$$\Delta^2 f(x,y) = \frac{1}{h^4}\begin{bmatrix} c_1 & c_2 & c_3 & c_4 & c_3 & c_2 & c_1 \\ c_2 & c_5 & c_6 & c_7 & c_6 & c_5 & c_2 \\ c_3 & c_6 & c_8 & c_9 & c_8 & c_6 & c_3 \\ c_4 & c_7 & c_9 & c_{10} & c_9 & c_7 & c_4 \\ c_3 & c_6 & c_8 & c_9 & c_8 & c_6 & c_3 \\ c_2 & c_5 & c_6 & c_7 & c_6 & c_5 & c_2 \\ c_1 & c_2 & c_3 & c_4 & c_3 & c_2 & c_1 \end{bmatrix} + \mathcal{O}(h^4). \tag{5.12}$$

General stencils are given by

$$c_4 = -\tfrac{1}{6} - 2c_1 - 2c_2 - 2c_3,$$

$$c_6 = -\tfrac{1}{6} - 54c_1 - 33c_2 - 6c_3 - 4c_5,$$

$$c_7 = \tfrac{7}{3} + 108c_1 + 64c_2 + 12c_3 + 6c_5,$$

$$c_8 = \tfrac{10}{3} + 351c_1 + 192c_2 + 30c_3 + 16c_5,$$

$$c_9 = -\tfrac{77}{6} - 594c_1 - 318c_2 - 50c_3 - 24c_5,$$

$$c_{10} = \tfrac{92}{3} + 976c_1 + 512c_2 + 80c_3 + 36c_5. \tag{5.13}$$

Isotropic stencils are given by

$$c_3 = -\tfrac{17}{180} - 9c_1 - 4c_2, \qquad c_4 = \tfrac{1}{45} + 16c_1 + 6c_2, \qquad c_5 = -\tfrac{29}{180} - 36c_1 - 12c_2,$$

$$c_6 = \tfrac{47}{45} + 144c_1 + 39c_2, \qquad c_7 = \tfrac{7}{30} - 216c_1 - 56c_2, \qquad c_8 = -\tfrac{187}{90} - 495c_1 - 120c_2,$$

$$c_9 = -\tfrac{191}{45} + 720c_1 + 170c_2, \qquad c_{10} = \tfrac{779}{45} - 1040c_1 - 240c_2. \tag{5.14}$$

For all isotropic stencils, the truncation error is $(7\,h^4/240)\,\Delta^4 f(x,y) + \mathcal{O}(h^6)$.

c_1	c_2	c_3	c_4	c_5	c_6	c_7	c_8	c_9	c_{10}	n_1	n_2
0	0	0	$-\frac{1}{6}$	$-\frac{1}{24}$	0	$\frac{25}{12}$	$\frac{8}{3}$	$-\frac{71}{6}$	$\frac{175}{6}$	21	29
											Ani
0	0	0	$-\frac{1}{6}$	0	$-\frac{1}{6}$	$\frac{7}{3}$	$\frac{10}{3}$	$-\frac{77}{6}$	$\frac{92}{3}$	25	25
											Ani
$-\frac{17}{1620}$	0	0	$-\frac{59}{405}$	$\frac{13}{60}$	$-\frac{7}{15}$	$\frac{5}{2}$	$\frac{187}{60}$	$-\frac{59}{5}$	$\frac{11431}{405}$	33	49
											Iso
0	0	$-\frac{17}{180}$	$\frac{1}{45}$	$-\frac{29}{180}$	$\frac{47}{45}$	$\frac{7}{30}$	$-\frac{187}{90}$	$-\frac{191}{45}$	$\frac{779}{45}$	37	37
											Iso

Ani, anisotropic; Iso, isotropic.

Shapes of these stencils from top to bottom:

F. $\mathcal{O}(h^2)$ Stencils for the Three-dimensional Bilaplacian

$$\Delta^2 f(x, y, z)$$

$$= \frac{1}{h^4} \begin{bmatrix} c_1 & c_2 & c_3 & c_2 & c_1 \\ c_2 & c_4 & c_5 & c_4 & c_2 \\ c_3 & c_5 & c_8 & c_5 & c_3 \\ c_2 & c_4 & c_5 & c_4 & c_2 \\ c_1 & c_2 & c_3 & c_2 & c_1 \end{bmatrix} \begin{bmatrix} c_2 & c_4 & c_5 & c_4 & c_2 \\ c_4 & c_6 & c_7 & c_6 & c_4 \\ c_5 & c_7 & c_9 & c_7 & c_5 \\ c_4 & c_6 & c_7 & c_6 & c_4 \\ c_2 & c_4 & c_5 & c_4 & c_2 \end{bmatrix} \begin{bmatrix} c_3 & c_5 & c_8 & c_5 & c_3 \\ c_5 & c_7 & c_9 & c_7 & c_5 \\ c_8 & c_9 & c_{10} & c_9 & c_8 \\ c_5 & c_7 & c_9 & c_7 & c_5 \\ c_3 & c_5 & c_8 & c_5 & c_3 \end{bmatrix} \begin{bmatrix} c_2 & c_4 & c_5 & c_4 & c_2 \\ c_4 & c_6 & c_7 & c_6 & c_4 \\ c_5 & c_7 & c_9 & c_7 & c_5 \\ c_4 & c_6 & c_7 & c_6 & c_4 \\ c_2 & c_4 & c_5 & c_4 & c_2 \end{bmatrix} \begin{bmatrix} c_1 & c_2 & c_3 & c_2 & c_1 \\ c_2 & c_4 & c_5 & c_4 & c_2 \\ c_3 & c_5 & c_8 & c_5 & c_3 \\ c_2 & c_4 & c_5 & c_4 & c_2 \\ c_1 & c_2 & c_3 & c_2 & c_1 \end{bmatrix}$$

$$+ \mathcal{O}(h^2). \tag{5.15}$$

General stencils are given by

$$c_7 = 2 - 32c_1 - 48c_2 - 16c_3 - 18c_4 - 8c_5 - 2c_6,$$

$$c_8 = 1 - 4c_1 - 8c_2 - 4c_3 - 4c_4 - 4c_5,$$

$$c_9 = 128c_1 + 188c_2 + 64c_3 + 64c_4 + 28c_5 + 4c_6 - 12,$$

$$c_{10} = 42 - 368c_1 - 528c_2 - 180c_3 - 168c_4 - 72c_5 - 8c_6. \tag{5.16}$$

Isotropic stencils are given by

$$c_1 = \tfrac{1}{24} - \tfrac{5}{4}c_2 - \tfrac{1}{2}c_3 - \tfrac{1}{4}c_4 - \tfrac{1}{8}c_5), \qquad c_6 = 32c_2 + 32c_3 + 4c_4 + 8c_5 - \tfrac{5}{3},$$

$$c_7 = 4 - 72c_2 - 64c_3 - 18c_4 - 20c_5, \qquad c_8 = \tfrac{5}{6} - 3c_2 - 2c_3 - 3c_4 - \tfrac{7}{2}c_5,$$

$$c_9 = -\tfrac{40}{3} + 156c_2 + 128c_3 + 48c_4 + 44c_5,$$

$$c_{10} = 40 - 324c_2 - 252c_3 - 108c_4 - 90c_5. \tag{5.17}$$

For all isotropic stencils, the truncation error is $(h^2/6)\,\Delta^3 f(x, y, z) + \mathcal{O}(h^4)$.

c_1	c_2	c_3	c_4	c_5	c_6	c_7	c_8	c_9	c_{10}	n_1	n_2	Stencil	Ref.
0	0	$\frac{1}{4}$	0	0	-1	0	0	0	5	21	67	Ani	
0	0	0	0	0	0	2	1	-12	42	25	25	Ani	11
$\frac{1}{24}$	0	0	0	0	$-\frac{5}{3}$	4	$\frac{5}{6}$	$-\frac{40}{3}$	40	41	125	Iso	
$-\frac{1}{36}$	0	0	$\frac{5}{18}$	0	$-\frac{5}{9}$	-1	0	0	10	52	125	Iso	
0	0	0	0	$\frac{1}{3}$	1	$-\frac{8}{3}$	$-\frac{1}{3}$	$\frac{4}{3}$	10	57	57	Iso	

Ani, anisotropic; Iso, isotropic.

Shapes of these stencils from top to bottom:
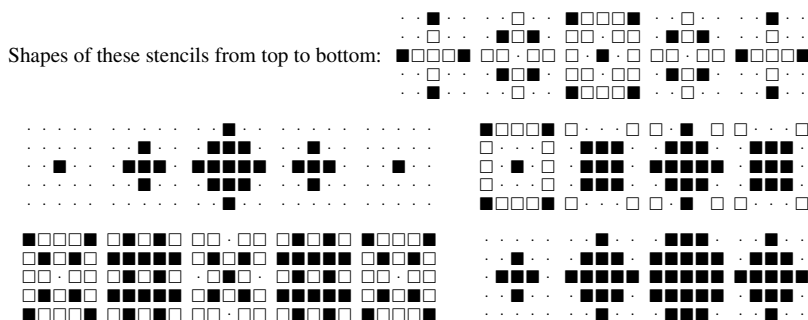
G. $\mathcal{O}(h^2)$ Stencils for the Gradient of a Two-dimensional Laplacian

$$\frac{d}{dx}\Delta f(x, y) = \frac{1}{h^3}\begin{bmatrix} c_1 & c_4 & 0 & -c_4 & -c_1 \\ c_2 & c_5 & 0 & -c_5 & -c_2 \\ c_3 & c_6 & 0 & -c_6 & -c_3 \\ c_2 & c_5 & 0 & -c_5 & -c_2 \\ c_1 & c_4 & 0 & -c_4 & -c_1 \end{bmatrix} + \mathcal{O}(h^2). \tag{5.18}$$

General stencils are given by

$$c_3 = \tfrac{1}{2} - 2c_1 - 2c_2, \qquad c_5 = \tfrac{1}{2} - 8c_1 - 2c_2 - 4c_4, \qquad c_6 = -2 + 16c_1 + 4c_2 + 6c_4. \tag{5.19}$$
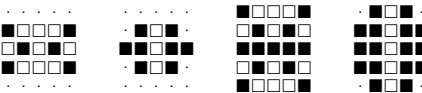
Isotropic stencils are given by

$$c_2 = \tfrac{1}{6} - 4c_1, \qquad c_3 = \tfrac{1}{6} + 6c_1, \qquad c_4 = \tfrac{1}{12} - 2c_1, \qquad c_5 = -\tfrac{1}{6} + 8c_1, \qquad c_6 = -\tfrac{5}{6} - 12c_1. \tag{5.20}$$

For all isotropic stencils, the truncation error is $(h^2/4)\frac{d}{dx}\Delta^2 f(x, y)$.

c_1	c_2	c_3	c_4	c_5	c_6	n_1	n_2	Stencil
0	$\frac{1}{4}$	0	0	0	-1	6	15	Ani
0	0	$\frac{1}{2}$	0	$\frac{1}{2}$	-2	8	12	Ani
$\frac{1}{24}$	0	$\frac{5}{12}$	0	$\frac{1}{6}$	$-\frac{4}{3}$	12	25	Iso
0	$\frac{1}{6}$	$\frac{1}{6}$	$\frac{1}{12}$	$-\frac{1}{6}$	$-\frac{5}{6}$	16	21	Iso

Ani, anisotropic; Iso, isotropic.

Shapes of these stencils from top to bottom:

H. $\mathcal{O}(h^4)$ Stencils for the Gradient of a Two-dimensional Laplacian

$$\frac{d}{dx}\Delta f(x, y) = \frac{1}{h^3}\begin{bmatrix} c_1 & c_5 & c_9 & 0 & -c_9 & -c_5 & -c_1 \\ c_2 & c_6 & c_{10} & 0 & -c_{10} & -c_6 & -c_2 \\ c_3 & c_7 & c_{11} & 0 & -c_{11} & -c_7 & -c_3 \\ c_4 & c_8 & c_{12} & 0 & -c_{12} & -c_8 & -c_4 \\ c_3 & c_7 & c_{11} & 0 & -c_{11} & -c_7 & -c_3 \\ c_2 & c_6 & c_{10} & 0 & -c_{10} & -c_6 & -c_2 \\ c_1 & c_5 & c_9 & 0 & -c_9 & -c_5 & -c_1 \end{bmatrix} + \mathcal{O}(h^4). \tag{5.21}$$

General stencils are given by

$$c_4 = -\tfrac{1}{8} - 2c_1 - 2c_2 - 2c_3, \qquad c_7 = -\tfrac{1}{12} - 36c_1 - 16c_2 - 4c_3 - 9c_5 - 4c_6,$$

$$c_8 = \tfrac{7}{6} + 72c_1 + 32c_2 + 8c_3 + 16c_5 + 6c_6,$$

$$c_{10} = -\tfrac{1}{24} - 18c_1 - 3c_2 - 12c_5 - 2c_6 - 6c_9,$$

$$c_{11} = \tfrac{5}{6} + 117c_1 + 32c_2 + 5c_3 + 48c_5 + 8c_6 + 15c_9,$$

$$c_{12} = -\tfrac{77}{24} - 198c_1 - 58c_2 - 10c_3 - 72c_5 - 12c_6 - 20c_9. \tag{5.22}$$

Isotropic stencils are given by

$$c_3 = -\tfrac{17}{240} - 9c_1 - 4c_2, \qquad c_4 = \tfrac{1}{60} + 16c_1 + 6c_2,$$

$$c_6 = -\tfrac{29}{360} - 24c_1 - 4c_2 - 6c_5, \qquad c_7 = \tfrac{47}{90} + 96c_1 + 16c_2 + 15c_5,$$

$$c_8 = \tfrac{7}{60} - 144c_1 - 24c_2 - 20c_5, \qquad c_9 = -\tfrac{17}{720} - 3c_1 - 2c_5,$$

$$c_{10} = \tfrac{47}{180} + 48c_1 + 5c_2 + 12c_5, \qquad c_{11} = -\tfrac{187}{360} - 165c_1 - 20c_2 - 30c_5,$$

$$c_{12} = -\tfrac{191}{180} + 240c_1 + 30c_2 + 40c_5. \tag{5.23}$$

For all isotropic stencils, the truncation error is $(7h^4/120)\frac{d}{dx}\Delta^2 f(x,y) + \mathcal{O}(h^6)$.

c_1	c_2	c_3	c_4	c_5	c_6	c_7	c_8	c_9	c_{10}	c_{11}	c_{12}
0	0	0	$-\frac{1}{8}$	0	$-\frac{1}{48}$	0	$\frac{25}{24}$	0	0	$\frac{2}{3}$	$-\frac{71}{24}$
						$n_1 = 14$		$n_2 = 27$		Ani	
0	0	0	$-\frac{1}{8}$	0	0	$-\frac{1}{12}$	$\frac{7}{6}$	0	$-\frac{1}{24}$	$\frac{5}{6}$	$-\frac{77}{24}$
						$n_1 = 18$		$n_2 = 23$		Ani	
$-\frac{17}{2160}$	0	0	$-\frac{59}{540}$	0	$\frac{13}{120}$	$-\frac{7}{30}$	$\frac{5}{4}$	0	$-\frac{7}{60}$	$\frac{187}{240}$	$-\frac{59}{20}$
						$n_1 = 26$		$n_2 = 49$		Iso	
0	0	$-\frac{17}{240}$	$\frac{1}{60}$	0	$-\frac{29}{360}$	$\frac{47}{90}$	$\frac{7}{60}$	$-\frac{17}{720}$	$\frac{47}{180}$	$-\frac{187}{360}$	$-\frac{191}{180}$
						$n_1 = 30$		$n_2 = 37$		Iso	

Ani, anisotropic; Iso, isotropic.

Shapes of these stencils from top to bottom:
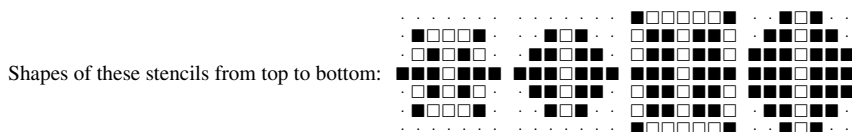
I. $\mathcal{O}(h^2)$ Stencils for the Gradient of a Three-dimensional Laplacian

$$\frac{\partial}{\partial x}\Delta f(x,y,z) = \frac{1}{h^3}
\begin{bmatrix} c_1 & c_7 & 0 & -c_7 & -c_1 \\ c_2 & c_8 & 0 & -c_8 & -c_2 \\ c_4 & c_9 & 0 & -c_9 & -c_4 \\ c_2 & c_8 & 0 & -c_8 & -c_2 \\ c_1 & c_7 & 0 & -c_7 & -c_1 \end{bmatrix}
\begin{bmatrix} c_2 & c_8 & 0 & -c_8 & -c_2 \\ c_3 & c_{10} & 0 & -c_{10} & -c_3 \\ c_5 & c_{11} & 0 & -c_{11} & -c_5 \\ c_3 & c_{10} & 0 & -c_{10} & -c_3 \\ c_2 & c_8 & 0 & -c_8 & -c_2 \end{bmatrix}
\begin{bmatrix} c_4 & c_9 & 0 & -c_9 & -c_4 \\ c_5 & c_{11} & 0 & -c_{11} & -c_5 \\ c_6 & c_{12} & 0 & -c_{12} & -c_6 \\ c_5 & c_{11} & 0 & -c_{11} & -c_5 \\ c_4 & c_9 & 0 & -c_9 & -c_4 \end{bmatrix}$$

$$\times
\begin{bmatrix} c_2 & c_8 & 0 & -c_8 & -c_2 \\ c_3 & c_{10} & 0 & -c_{10} & -c_3 \\ c_5 & c_{11} & 0 & -c_{11} & -c_5 \\ c_3 & c_{10} & 0 & -c_{10} & -c_3 \\ c_2 & c_8 & 0 & -c_8 & -c_2 \end{bmatrix}
\begin{bmatrix} c_1 & c_7 & 0 & -c_7 & -c_1 \\ c_2 & c_8 & 0 & -c_8 & -c_2 \\ c_4 & c_9 & 0 & -c_9 & -c_4 \\ c_2 & c_8 & 0 & -c_8 & -c_2 \\ c_1 & c_7 & 0 & -c_7 & -c_1 \end{bmatrix}
+ \mathcal{O}(h^2). \tag{5.24}$$

General stencils are given by

$$c_6 = \tfrac{1}{2} - 4c_1 - 8c_2 - 4c_3 - 4c_4 - 4c_5,$$

$$c_{11} = \tfrac{1}{2} - 16c_1 - 20c_2 - 4c_3 - 8c_4 - 2c_5 - 8c_7 - 10c_8 - 4c_9 - 2c_{10},$$

$$c_{12} = -3 + 64c_1 + 80c_2 + 16c_3 + 32c_4 + 8c_5 + 28c_7 + 32c_8 + 12c_9 + 4c_{10}. \tag{5.25}$$

Isotropic stencils are given by

$$c_5 = \tfrac{1}{6} - 8c_1 - 10c_2 - 2c_3 - 4c_4, \qquad c_6 = -\tfrac{1}{6} + 28c_1 + 32c_2 + 4c_3 + 12c_4,$$

$$c_8 = \tfrac{1}{32} - 4c_1 - 2c_2 - \tfrac{1}{4}c_3 - 2c_7 - \tfrac{1}{8}c_{10}, \qquad c_9 = \tfrac{1}{48} + 4c_1 + \tfrac{1}{2}c_3 - 2c_4 + 2c_7 + \tfrac{1}{4}c_{10},$$

$$c_{11} = -\tfrac{11}{48} + 24c_1 + 20c_2 + \tfrac{1}{2}c_3 + 8c_4 + 4c_7 - \tfrac{7}{4}c_{10},$$

$$c_{12} = -\tfrac{5}{12} - 80c_1 - 64c_2 - 2c_3 - 24c_4 - 12c_7 + 3c_{10}. \qquad (5.26)$$

For all isotropic stencils, the truncation error is $(h^2/4)\frac{d}{dx}\Delta^2 f(x,y) + \mathcal{O}(h^6)$.

c_1	c_2	c_3	c_4	c_5	c_6	c_7	c_8	c_9	c_{10}	c_{11}	c_{12}	n_1	n_2	Stencil
0	0	$\tfrac{1}{8}$	0	0	0	0	0	0	0	0	-1	10	23	Ani
0	0	0	0	0	$\tfrac{1}{2}$	0	0	0	0	$\tfrac{1}{2}$	-3	12	17	Ani
0	0	0	$\tfrac{1}{24}$	0	$\tfrac{1}{3}$	0	0	0	$\tfrac{1}{4}$	$-\tfrac{1}{3}$	$-\tfrac{2}{3}$	28	57	Iso
0	0	0	0	$\tfrac{1}{6}$	$-\tfrac{1}{6}$	0	0	$\tfrac{1}{12}$	$\tfrac{1}{4}$	$-\tfrac{2}{3}$	$\tfrac{1}{3}$	36	49	Iso

Ani, anisotropic; Iso, isotropic.

Shapes of these stencils from top to bottom:
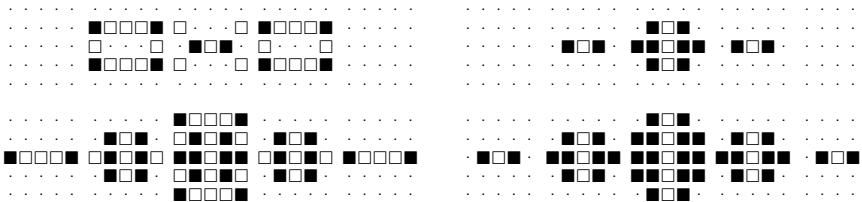
VI. COMPUTATIONAL CONSIDERATIONS

A naive picture of a computer suggests that it has a certain amount of homogeneous memory. In reality, only a small part of the memory, known as cache, is able to supply data to the cpu at a speed comparable to the speed at which the cpu can perform floating-point operations. (Modern computers have different levels of caches but we will ignore this complication here.) The speed of moving data between main memory and cache can thus be the speed-limiting factor. Let us assume that the cache is able to hold M floating point numbers.

We want to apply a differential operator D to a function $f(\vec{x})$ over the entire spatial region $\vec{x} \in \Omega \equiv [0; (N-1)h]^d$, where d is the dimension ($d = 2, 3$) and h is the grid spacing. The list of function values $f(\vec{x})$ can thus be stored as a matrix A containing N^d elements. If $M \geq 2N^d$ this can be done entirely inside the cache. (The factor 2 appears because the result also has to be stored somewhere. The memory needed for the coefficients of the stencil is negligible.) The computing time needed is then practically proportional to the number of floating point operations, and thus practically proportional to the number of nonzero elements n_1 of the stencil.

If A no longer entirely fits into the cache, parts of A are loaded into the cache, are then processed and then discarded from the cache again. If A is traversed in some sensible order, most of the cache entries are used several times before they are replaced with new data. (This is the reason why arrays in Fortran should have their left-most index vary fastest, whereas in C it should be the right-most index. Professional linear algebra packages such as LAPACK [12] use algorithms known as blocked algorithms specially designed to take account of finite cache size.) To process the entire

matrix A, each element of it is loaded into the cache once only if the condition $M \geq (2r+1)N^{d-1}$ is fulfilled. (Remember that $2r+1$ is the width of the stencil.) Assuming that loading data into the cache from normal memory takes much longer than typical floating-point cpu operations, the computing time becomes independent of the stencil.

In addition to the throughput considerations described above, the question of latencies is also important. The maximal throughput is determined by the hardware and cannot be increased by software means. Latencies, in contrast, can be reduced by issuing prefetch commands for pieces of data some time before they are actually needed. Modern compilers are able to perform prefetching (unfortunately, the benefit varies).

To check the speed of the stencils derived in this article, we have implemented the Laplacian and the Bilaplacian (because they are the most commonly used) on three different systems, namely a SparcStation Ultra 60 (450 MHz UltraSparc processors), an AlphaServer ES45 (1 GHz EV6.8CB processors) and an Intel Pentium IV computer (3 GHz). For the first two systems, the program was written in Fortran 90 and compiled with highest optimisation using the native compilers supplied by the vendors. For the Intel system, we used SSE2 intrinsics to increase the speed of the program, and compilation was done using the Intel compilers at standard optimisation. For each computer system, the time needed to compute $\mathcal{S}f(\vec{x})$ for all $\vec{x} \in \Omega$ using the fastest anisotropic and the fastest isotropic stencil was measured as a function of matrix size N. Periodic boundary conditions were applied:

$$f(0, y, z) = f(Nh, y, z), \qquad f(x, 0, z) = f(y, Nh, z), \qquad \cdots . \tag{6.1}$$

The ratio of those two times quantifies the extra cost of using an isotropic stencil.

The graphs for the Laplacian in Fig. 2 show an effect of finite cache size that agrees very well with the theoretical throughput argument presented above. Although the matrix still fits into the cache, the speed of the algorithm depends on the complexity of the stencil. After that, the speed
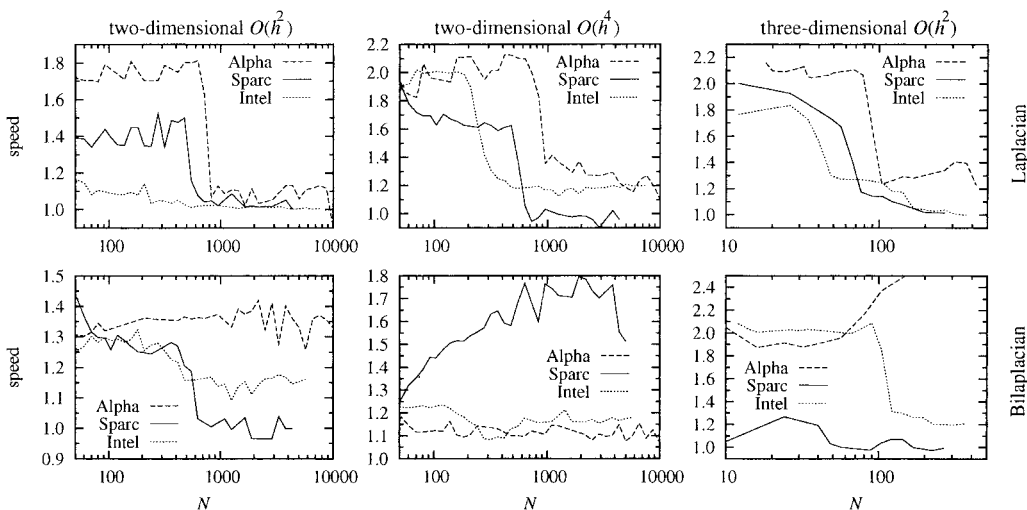

FIG. 2.   Ratio of the time needed for the fastest isotropic stencil and the fastest anisotropic stencil with the same order. A value of "1.6" means that the isotropic stencil needs 60% longer to compute than the anisotropic stencil. Data for the Laplacian (top) and the Bilaplacian (bottom) are shown for (from left to right) two-dimensional $\mathcal{O}(h^2)$, two-dimensional $\mathcal{O}(h^4)$, and three-dimensional $\mathcal{O}(h^2)$ stencils; see also the labels on the top and on the right.

becomes almost independent of the stencil, as reloading the cache becomes the limiting step. The different cache sizes of the different processors are seen very clearly.

For the Bilaplacian, the situation is a bit different (see Fig. 2) due to strange behavior of the compilers. For some combinations of N and stencil $\mathcal{S}$, the speed of the generated executable is even much lower than for slightly larger or smaller N. (It should be stressed that the "noise" in the figures is caused by this and is thus reproducible. We only used values of N that were multiples of 8 to ensure that complete cache lines would be used.) We do not believe that a deeper discussion of this would be fruitful. We rather encourage the reader to check the behavior with their own hardware and their own compilers at different optimization levels because they might behave very differently from the computers that we used.

The main conclusion from Fig. 2 is that for large enough matrices the extra cost for using isotropic stencils for Laplacian and Bilaplacian usually is no more than 20%—even though the stencils may contain more than twice as many elements. All current research studies systems that no longer fit into the cache, so that those simulations are in the large-matrix regime. We may thus conclude that there is little reason to use an anisotropic stencil in favour of an isotropic stencil of the same order.

VII. DISCUSSION

As could be seen from the references given in Section V, only a few of the stencils have been published before. This simply reflects the fact that most of the work geared toward stencils has focused on solving PDEs with boundary conditions of type (1.1), with recent work focusing on "higher-order compact stencils." We want to comment shortly on the connection between such stencils and the isotropic stencils presented in this articles.

The leading error term of the isotropic stencils presented in this article, described by the differential operator $\tilde{\mathcal{D}}$, is, by definition, isotropic. However, $\tilde{\mathcal{D}}$ has the additional property that it can be expressed with help of the original differential operator $\mathcal{D}$. This is best explained by an example. For the isotropic $\mathcal{O}(h^2)$ stencils for the Laplacian presented in this article, one has (cf. Section VA)

$$\Delta f(x, y) = \mathcal{S}f(x, y) + dh^2\Delta^2 f(x, y) + \mathcal{O}(h^4), \tag{7.1}$$

i.e., the relation between $\mathcal{D}$ and $\tilde{\mathcal{D}}$ is $\tilde{\mathcal{D}} = \mathcal{D}^2$. Using this finite-difference scheme to solve the boundary condition PDE

$$\Delta g(x, y) = \rho(x, y), \tag{7.2}$$

for the unknown function $g(x, y)$ from the known function $\rho(x, y)$ gives

$$\mathcal{S}g(x, y) + dh^2\Delta^2 g(x, y) + \mathcal{O}(h^4) = \rho(x, y). \tag{7.3}$$

The essential point now is that the lowest-order truncation error $\Delta^2 g(x, y)$ can be evaluated using the original differential equation (7.2) to give $\Delta\rho(x, y)$, and the latter can be expressed using Eq. (7.1) as $\mathcal{S}\rho(x, y)$, yielding

$$\mathcal{S}g(x, y) + dh^2\mathcal{S}\rho(x, y) + \mathcal{O}(h^4) = \rho(x, y). \tag{7.4}$$

Even though $\mathcal{S}$ is only an $\mathcal{O}(h^2)$ stencil, Eq. (7.4) is exact to $\mathcal{O}(h^4)$.

The result is of higher order because it was possible to evaluate the leading error term of the unknown $g(x, y)$ from a differential operator acting on the known $\rho(x, y)$, thereby eliminating this error term. This is the basic idea behind higher-order compact stencils. Because this is possible for all compact isotropic stencils derived in this article, all of them qualify as higher-order compact stencils.

The noncompact isotropic stencils found in this article can be used in a similar manner to arrive at results for boundary condition PDEs having a truncation error of higher order than the order of the used stencil. Unfortunately, this is of little practical use: The linear-equation solver needed for Eq. (7.4) works very inefficiently unless the stencil is diagonally dominant [1, pp 122 and 158; 2, p 151]. Due to this, the new isotropic stencils (which are all noncompact and nondiagonally dominant) presented in this article are relevant only for initial-condition problems of type (1.4).

For the Bilaplacian no compact explicit stencils exist, and for boundary-condition problems of type (1.1) numerical difficulties consequently arise already in two dimensions [13, 14]. The advantage offered by compact diagonally dominant stencils is so large that most of the previous work on the Bilaplacian has focused on introducing auxiliary variables, such that the stencils applied on those auxiliary variables remain compact. The first possibility is to split $\Delta^2 f = \rho$ into the two equations $\Delta f = u, \Delta u = \rho$ (see e.g., Refs. 15–17 and references therein). The second option is to introduce the gradients of f in all spatial directions as additional variables (see Ref. 17 for 2D and Ref. 18 for 3D). For boundary-condition problems, this is the advisable way to go. For initial-condition problems, however, using one of the novel isotropic stencils presented in this article is much more efficient and straightforward. Due to the significant pen-and-paper work, the 25-point formula for the three-dimensional Bilaplacian was, to the best of our knowledge, published only in 1967 [11] (the stencil is reprinted, e.g., in Ref. 18), and the other stencils have not been reported before.

VIII. CONCLUSIONS

In this article, we have presented different stencils for the Laplacian, the Bilaplacian, and the gradient of the Laplacian, designed for initial value problems. The stencils are also available as a Mathematica file that includes routines to verify that the coefficients indeed correspond to correct stencils. Using that file avoids the risk of typos.

The focus of our article is on isotropic stencils, i.e., on stencils where the truncation error does not depend on the choice of the coordinate system. These stencils contain significantly more elements than the traditionally used anisotropic stencils. We have shown, however, that in most situations the limited speed of data transfer between memory and cache leads to a decrease in speed of no more than 20% when isotropic stencils are used instead of anisotropic ones. This small price to pay means that there are only few situations where anisotropic stencils should still be used for initial value problems. We hope that our work will encourage the use of isotropic stencils in wider areas of science than it is done at the moment.

References

1. B. Wendroff, Theoretical numerical analysis, Academic Press, London, 1966.

2. G. Sewell, The numerical solution of ordinary and partial differential equations, Academic Press, London, 1988.

3. H. B. Keller and V. Pereyra, Symbolic generation of finite difference formulas, Math Comput 32 (1978), 955–971.

4. Tony Shardlow, Splitting for dissipative particle dynamics, SIAM J Sci Comp 24 (2003), 1267–1282.

5. James D. Murray, Mathematical biology, Springer, Berlin, 1993.

6. P. C. Hohenberg and B. I. Halperin, Theory of dynamical critical phenomena, Rev Mod Phys 49 (1977), 435–479.

7. M. Abramowitz and I. A. Stegun, Handbook of mathematical functions, Dover, New York, 1970.

8. M. M. Gupta and J. Kouatchou, Symbolic derivation of finite difference approximations for the three-dimensional Poisson equation, Numer Meth Part Diff Eq 14 (1998), 593–606.

9. U. Ananthakrishnaiah, R. P. Manohar, and J. W. Stephenson, Fourth-order finite difference methods for three-dimensional general linear elliptic problems with variable coefficients, Num Meth Part Diff Eq 3 (1987), 229–240.

10. W. F. Spotz and G. F. Carey, A high-order compact formulation for the 3D Poisson equation, Numer Meth Part Diff Eq 12 (1996), 235–243.

11. J. R. Dos Santos, Équations aux différences finies pour l'équation biharmonique dans l'espace à trois dimensions, CR Acad Sci Paris Sér A–B 264 (1967), A291–A293.

12. E. Anderson, Z.-J. Bai, C. Bischof, L. S. Blackford, J. Demmel, J. Dongarra, J. du Cro, A. Greenbaum, S. Hammarling, A. McKenney, and D. Sorensen, LAPACK Users' Guide, 3rd. ed., SIAM, Philadelphia, 1999.

13. S. D. Conte and R. T. Dames, On an alternating direction method for solving the plate problem with mixed boundary conditions, J Assoc Comput Mach 7 (1960), 264–273.

14. M. M. Gupta and R. P. Manohar, Direct solution of the biharmonic equation using noncoupled approach, J Comput Phys 33 (1979), 236–248.

15. M. M. Gupta, Discretization error estimates for certain splitting procedures for solving first biharmonic boundary value problems, SIAM J Numer Anal 12 (1975), 364–377.

16. R. Glowinski and O. Pironneau, Numerical methods for the first biharmonic equations and for the two-dimensional Stokes problem, SIAM Rev 21 (1979), 167–212.

17. I. Altas, J. Dym, M. M. Gupta, and R. P. Manohar, Multigrid solution of automatically generated high-order discretizations for the biharmonic equation, SIAM J Sci Comput 19 (1998), 1575–1585.

18. I. Altas, J. Erhel, and M. M. Gupta, High accuracy solution of the three-dimensional biharmonic equations, Num Algorithms 29 (2002), 1–19.